0273-2289/98/70–72—0037$11.50

Shrinking-Bed Model for Percolation Process Applied to Dilute-Acid Pretreatment/Hydrolysis of Cellulosic Biomass

RONGFU CHEN, ZHANGWEN WU, AND Y. Y. LEE*

Department of Chemical Engineering, Auburn University, AL 36849

ABSTRACT

For many lignocellulosic substrates, hemicellulose is biphasic upon dilute-acid hydrolysis, which led to a modified percolation process employing simulated two-stage reverse-flow. This process has been proven to attain substantially higher sugar yields and concentrations over the conventional single-stage percolation process. The dilute-acid pretreatment of biomass solubilizes the hemicellulose fraction in the solid biomass, leaving less solid biomass in the reactor and reducing the bed. Therefore, a bed-shrinking mathematic kinetic model was developed to describe the two-stage reverse-flow reactor operated for hydrolyzing biphasic substrates, including hemicellulose, in corn cob/stover mixture (CCSM). The simulation indicates that the shrinking-bed operation increases the sugar yield by about 5%, compared to the nonshrinking bed operation in which 1 reactor volume of liquid passes through the reactor (i.e., $\tau = 1.0$). A simulated optimal run further reveals that the fast portion of hemicellulose is almost completely hydrolyzed in the first stage, and the slow portion of hemicellulose is hydrolyzed in the second stage. Under optimal conditions, the bed shrank 27% (a near-maximum value), and a sugar yield over 95% was attained.

Index Entries: Dilute-acid pretreatment; modeling; shrinking bed; percolation; corn cobs/stover mixture.

INTRODUCTION

Pretreatment is necessary to bioconvert lignocellulosic biomass into fuels and chemicals. Pretreatment with dilute sulfuric acid is a viable process option; however, a concern is that the sugars decompose under high temperature and low pH to form undesirable components that are toxic in the subsequent fermentation. To avoid this, it is important to select

* Author to whom all correspondence and reprint requests should be addressed.

proper reaction conditions, reactor configurations, and operation conditions. Previous studies *(1–4)* have established that a percolation reactor (packed-bed, flow-through type) is most suitable for biomass pretreatment, because the sugar products are discharged from the reactor as they form, thus reducing sugar decomposition. High sugar concentrations can also be attained because of the high solid-to-liquid ratio that exists in a packed-bed reactor. In the previous bench-scale modeling and experimental work *(5,6)*, it was demonstrated that a two-stage, two-temperature, reverse-flow scheme significantly enhances the overall performance of the percolation reactor. It simulates countercurrent flow of the biomass solid and hydrolysis liquor, and it exploits the fact that hemicellulose exhibits a biphasic behavior upon dilute acid hydrolysis. A low temperature is applied in the first stage to hydrolyze the labile xylan, then a high temperature is applied in the second stage to hydrolyze the resilient xylan.

Acid pretreatment solubilizes the hemicellulose in biomass. In previous modeling work *(5)*, to retain the linearity of the governing equations, the authors assumed that the bulk-packing volume of the solid biomass in the reactor remained constant during the hydrolysis. This was done to retain the linearity of the governing equations. However, in actual operation, the bulk-packing density of the solid biomass in the reactor changes because of the solubilization of the hemicellulose, which leaves less solid biomass in the reactor. To further optimize the pretreatment process, a shrinking-bed reactor was proposed by NREL *(7)*. It was designed to keep a constant bulk-packing density of the solid biomass in the reactor, so that the high solid-to-liquid ratio would allow a high product concentration to be obtained. Figure 1 shows a simplified diagram of a bench-scale, shrinking-bed, percolation reactor. The reactor has a fixed and a movable end; the movable end is supported by a compressed spring. As the reaction progresses, the gradual depletion of the packed-solid biomass causes the particle structure to be less dense. To overcome this limitation, the spring-attached movable end presses the loose biomass particles closer, allowing the bulk-packing density of the lignocellulosic biomass to be maintained constant. Although pilot-scale reactor designs, which allow for the continual shrinkage of the biomass-bed as a function of hydrolysis, will most likely not resemble the bench-scale design (Fig. 1), it is instructive to model the shrinking-bed concept for subsequent design. In this work, process modeling and simulation were performed for this shrinking-bed reactor as it applies to the acid hydrolysis of lignocellulosic.

This investigation establishes a process model for the shrinking-bed reactor, which prehydrolyzes the hemicellulose in a corn cobs/stover mixture (CCSM). The modeling work is directed toward optimal operation of the shrinking-bed reactor and analysis on the bed-shrinking phenomena. The issues addressed in the modeling and simulation are the extent and the effect of bed-shrinking, substrate variation in the reactor, and product yield and concentration.

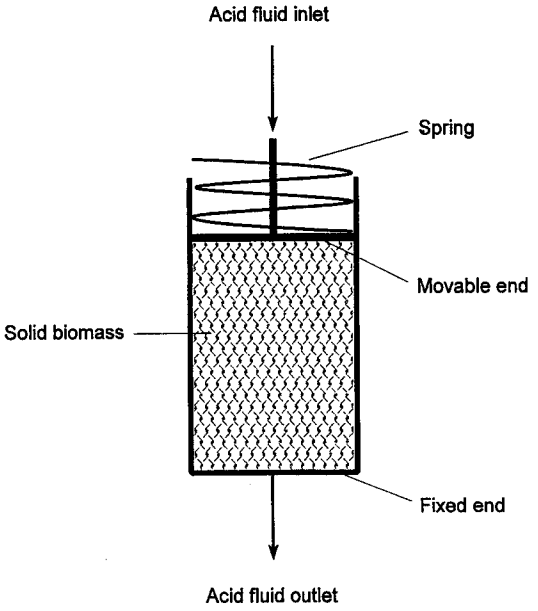

Fig. 1. A simplified diagram of a shrinking-bed reactor applied in pretreatment.

MODEL DEVELOPMENT

The shrinking-bed percolation reactor has a solid bed that shrinks during hydrolysis because of hemicellulose solubilization (Fig. 1). The effective reactor volume (or the length of solid bed of biomass in the percolation reactor) is related to hemicellulose conversion. For a differential value of τ^i, or a differential amount of acid fluid, the percolation process is assumed to be a nonshrinking-bed reactor, because a differential amount of hemicellulose is removed during that time span. The nonshrinking process is then followed by a compression stage, in which the biomass is compressed to its original packing density. It is assumed that no reaction occurs in this stage. The model for the shrinking-bed reactor can be decoupled, as shown in Figure 2, by repeating the operation of nonshrinking-bed reaction with a differential amount of liquid τ^i followed by a compression process. Adoption of this method allows the governing partial differential equations to be linear; therefore, the analytical solution previously obtained for nonshrinking-bed operation (5) directly applies to the present case.

A shrinking factor (ξ^i) is defined as the ratio of the reactor volume after the *i*th compression operation to that before the *i*th compression operation.

$$\xi^i = V^i/V^{i-1} \tag{1}$$

For the cylindrical reactor, Eq. 1 can also be expressed in terms of reactor length:

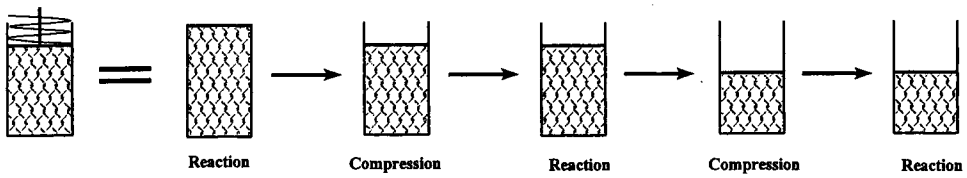

Fig. 2. Decomposition of a shrinking-bed reactor operation.

$$\xi^i = L^i/L^{i-1} \tag{2}$$

The shrinking factor ξ^i (≤ 1) is a function of hemicellulose conversion only.

The conversion (θ^i) of hemicellulose during one differential value of τ^i is

$$\theta^i = H^{i-1} - H^i/H^{i-1} \tag{3}$$

which is valid only for the nonshrinking-bed operation. The hemicellulose concentration in the reactor H^{i-} and H^i are determined by Eq. 8 in ref. *5*.

The composition (η^i) of hemicellulose in the solid biomass changes during the hydrolysis, as hemicellulose and some lignin are solubilized into the hydrolyzate. It can, based on material balance, be expressed as

$$\eta^i = \frac{\eta^{i-1}(1 - \theta^i)}{1 - \eta^{i-1}\theta^i(1 + r)} \tag{4}$$

where γ is the ratio of solubilized lignin to solubilized hemicellulose and cellulose during the pretreatment. It is assumed to be constant throughout the reaction. For the sample substrate of CCSM, with 20.0% xylan, 39.2% glucan, and 23.3% lignin *(8)*, it was assumed that 80% of total lignin was dissolved with the solubilization of hemicellulose and cellulose. Therefore, the γ value is calculated to be 0.315 from the composition of the feedstock.

The change of reactor volume resulting from the solubilization of hemicellulose and lignin is expressed as

$$V^i = V^{i-1}[1 - \eta^{i-1}\,\theta^{i-1}\,(1 + \gamma)] \tag{5}$$

Therefore, the shrinking factor is determined by

$$\xi^i = 1 - \eta^{i-1}\,\theta^i\,(1 + \gamma) \tag{6}$$

for one stage of compression operation.

The overall reaction conversion ($\theta_{overall}$) after the nth nonshrinking and compression operations, based on the initial reaction conditions, is expressed as:

$$\theta_{\gg\wedge\supset\oplus\nwarrow LL} = 1 - \frac{H_{\ll}}{H_{\gg}} \prod_{i=1}^{\ll} \xi^i \tag{7}$$

Similarly, the overall length of the shrinking-bed reactor during the reactions is:

$$L = L_{\gg} \prod_{i=1}^{\ll} \xi^i \tag{8}$$

The overall yield is determined by summing the yields from the nonshrinking-bed model with consideration of the compression operation. It is then expressed as:

$$Y_{\Theta} = \frac{1}{H_{\gg}} \sum_{\Gamma=1}^{\ll} (Y^{\Gamma}{}_{\ll\Theta} H^{\Gamma} \prod_{i=1}^{\ll} \xi^{\Gamma} \tag{9}$$

where Y_s = sugar yield from shrinking-bed operation,
Y_{ns} = sugar yield from nonshrinking-bed operation *(5)*,
H_0 = initial concentration of hemicellulose as xylose in the reactor,
j = 1, 2, ... n, and
i = 1, 2, ... j.

RESULTS AND DISCUSSION

The shrinking-bed operation is similar to the nonshrinking-bed operation, except there is a compression step between each differential reaction period τ^i. The compression process increases the solid-packing density to its previous level, but does not change the biomass composition; therefore, the optimum temperature profile previously determined for the nonshrinking operation is also applied to the shrinking-bed operation. In the shrinking-bed reactor, the bed depth changes during the reaction; therefore, the optimum flow rate must be adjusted to respond to the reduced liquid residence time. The computational modeling work was done for CCSM. The two-stage, reverse-flow operation (Fig. 3A) is identical in theory to the process shown in Figure 3B *(5)*, so the shrinking-bed process was modeled based on the scheme of Figure 3B.

Effect of Acid Flow Rate and τ

In the previous nonshrinking-bed model, the optimal flow rate is obtained for a given reactor length at particular temperature *(5)*. The dimensionless reaction rate β_i ($= l_i L/u$) is an optimized operational parameter. If the length of the reactor is reduced, the flow rate of the liquid u should also be reduced to maintain β at its optimum. However, this opera-

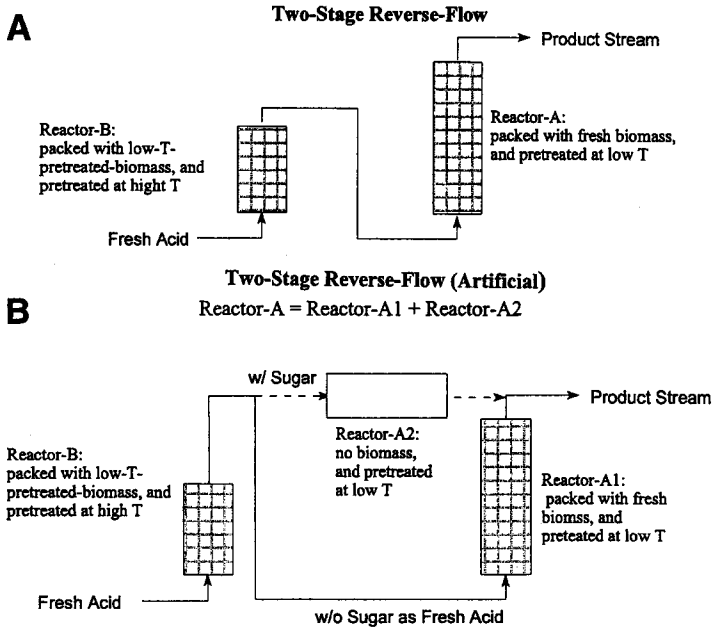

Fig. 3. Schematics of temperature step-change, two-stage, reverse flow, and shrinking-bed operation.

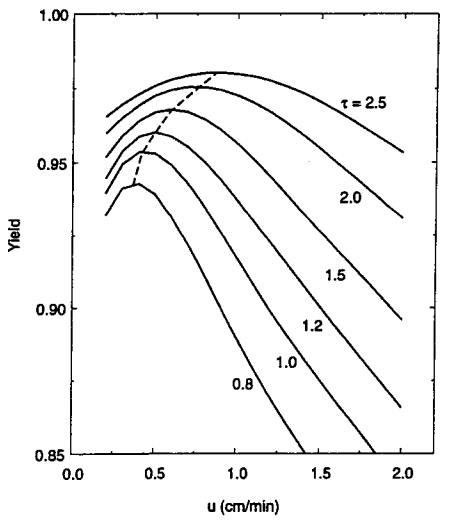

Fig. 4. Effect of acid flow rate on sugar yield at various τ values. (Two-stage, reverse-flow, shrinking-bed mode, T_1 = 140°C, T_2 = 170°C, L_o = 15.24 cm, C_o = 3.33 w/v%, and acid concentration = 0.8 wt%.)

tion is not convenient in practice. The authors have studied the effect of acid flow rate on sugar yield at a constant flow-rate operation. Figure 4 shows the effect of flow rate on sugar yield at the optimum temperature step change (140–170°C) (*5*). For a given τ, there is an optimum u to obtain

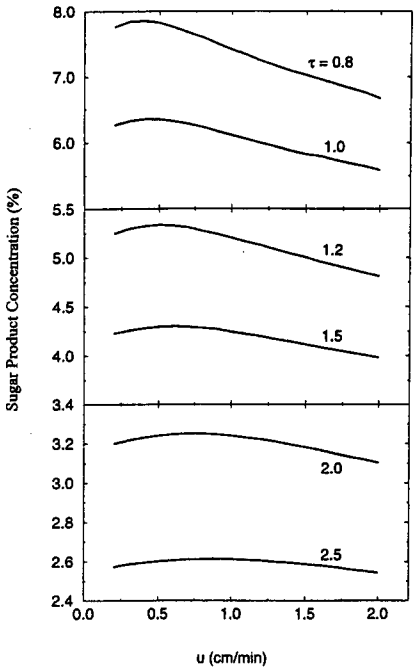

Fig. 5. Effect of acid flow rate on sugar product concentration (Cp) at various τ values. (Two-stage, reverse-flow, shrinking-bed mode, T_1 = 140°C, T_2 = 170°C, L_o = 15.24 cm, C_o = 3.333 w/v%, and acid concentration = 0.8%).

the maximum yield. For τ = 0.8, the maximum yield of 0.94 is obtained at u = 0.4 cm/min; at τ = 2.5, the maximum yield of 0.98 is obtained at u = 0.8. High τ-values give high sugar yields; however, high τ lowers the sugar concentration in the hydrolysate, as clearly shown in Figure 5. With application of the respective optimum flow rates, the maximum sugar concentrations are 7.8% at τ = 0.8 and 2.6% at τ = 2.5. Obviously, there is a trade-off between yield and sugar concentration. A proper choice of τ can only be made considering the overall process economics.

Comparison Between Shrinking-Bed and Nonshrinking-Bed Operations

One advantage of the shrinking-bed operation, over the nonshrinking one, is that τ becomes higher, even for the same amount of liquid throughput. Consider a shrinking-bed reactor with an initial volume the same as that of a nonshrinking-bed reactor. For τ = 1, this means one reactor volume of liquid has passed through the nonshrinking bed reactor during the reaction. For the shrinking-bed operation, if, for example, 50% of the biomass dissolves, 1 reactor volume of liquid at the initial phase of the reaction will become 2 reactor volumes at the latter phase. Because yield increases with τ (fluid input into the reactor) at a given temperature and

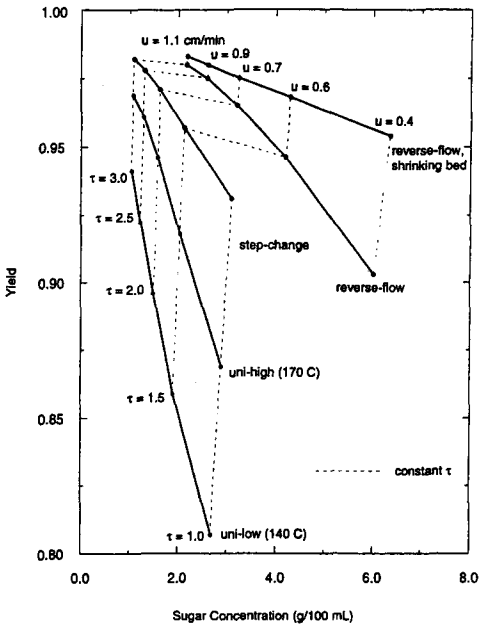

Fig. 6. Yield and sugar product concentration under various operation modes. (Acid concentration = 0.8%, C_o = 3.333 w/v%, u = optimum values for shrinking-bed operation).

flow rate, the shrinking-bed operation is expected to give a higher yield. Figure 6 compares the shrinking-bed and nonshrinking-bed operations, both with temperature-step-change, reverse-flow operations, and uniform temperature operations. It shows that the shrinking-bed operation gives the highest sugar yield for a given τ. The sugar yield increases about 5% at τ = 1.0, 2% at τ = 1.5, and 0.2% at τ = 3.0 over those from nonshrinking-bed, step-change, reverse-flow operation modes. The sugar concentration from the shrinking-bed operation is slightly higher than that of the non-shrinking-bed operation.

Overall Hemicellulose Conversion

Figure 7 shows the profile of hemicellulose conversion during a two-stage shrinking-bed operation with τ = 1.5 for various flow rates. As shown in Figure 4, the flow rates of 0.2 and 2.0 cm/min are the lower and upper limits of this work, and a flow rate of 0.6 cm/min is the optimal value for τ = 1.5. Figure 7 indicates that a low flow-rate of 0.2 cm/min induces an excessive residence time, causing overreaction and significant decomposition. The reaction achieves near-complete conversion at about τ = 1; however, the sugar yield is about 0.95, and sugar loss, about 5%. On the other hand, with the flow rate of 2.0 cm/min, the hemicellulose conversion is only 91%, and the sugar yield is 0.90. Loss of sugar because of decomposition is therefore about 1%. With the flow rate of 0.6, the hemicellulose conversion is in excess of 99%, and the yield is 0.97, thus

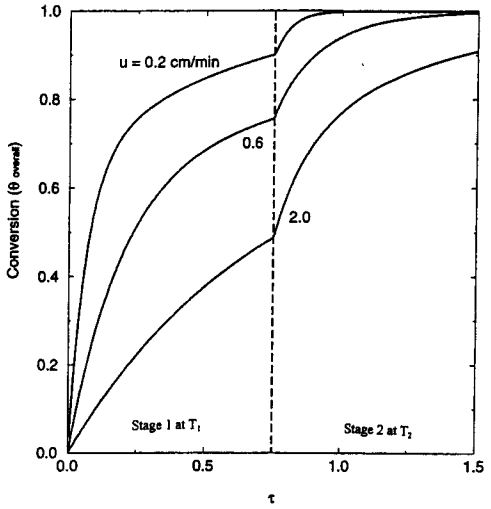

Fig. 7. The extent of hemicellulose conversion ($\theta_{overall}$) at various flow rate (u). (T_1 = 140°C, T_2 = 170°C, L_o = 15.24 cm, C_o = 3.333 w/v%, and acid concentration = 0.8%).

causing about 2% sugar loss. It is also seen that 75% conversion of hemicellulose was achieved in the first stage alone (low-temperature stage).

Distribution of Fast and Slow Portions of Hemicellulose During Hydrolysis

A two-stage temperature-step-change operation is particularly beneficial for hydrolysis of biphasic hemicellulose. In the overall process scheme, the fast portion of the hemicellulose is hydrolyzed at low temperature and the slow portion of hemicellulose at a high temperature. In a previous kinetic study *(5)*, it was determined that the fast portion of hemicellulose in CCSM is 65%. Figure 8 shows the distribution of fast and slow portions of hemicellulose in the two-stage reactor at optimum temperature-step-change (140–170°C) condition *(5)*. Three flow-rate conditions of 0.2, 0.6, and 2.0 cm/min, at τ = 1.5, were applied in the study. For the case of u = 0.2 cm/min, the fast portion of hemicellulose was quickly dissolved at the early stage, at τ less than 0.5, and about 60% of the slow portion of hemicellulose was hydrolyzed after the first stage. The remaining slow portion of hemicellulose was completely hydrolyzed in the second stage, with a final sugar yield of 0.95. For u = 2.0, only about 60% of the fast portion and no slow portion of hemicellulose were hydrolyzed after the first stage. The remaining fast portion and about 61% of the slow portion of hemicellulose were dissolved after the second stage, giving a sugar yield of only 0.90, because of incomplete hydrolysis. With u = 0.6 and τ = 1.5 (the optimum point), about 97% of the fast portion and 19% of the slow portion of were hydrolyzed after the first stage. The remainder of the fast portion and 99% of the slow portion were hydrolyzed after the second stage, to give the total of 97% yield.

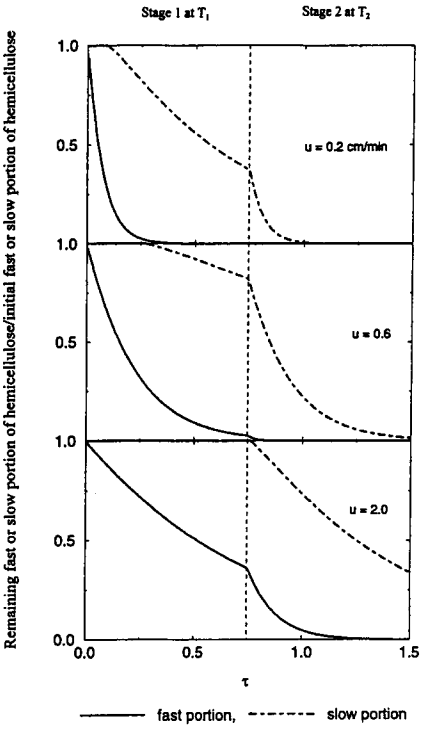

Fig. 8. Effect of acid flow rate (u) on the remaining fast or slow portion of hemicellulose. (T_1 = 140°C, T_2 = 170°C, L_o = 15.24 cm, C_o = 3.333 w/v%, and acid concentration = 0.8%).

Bed-Shrinking During Hydrolysis

In the bed-shrinking model, the shrinking process is terminated when the hydrolysis of hemicellulose is completed. Figure 9 shows the extent of shrinkage for the period of τ = 1.5 at various liquid flow rates (u). For the flow rate of 0.2 cm/min, the shrinking process was terminated at about τ = 1.0, because of complete hydrolysis. At the termination, the total bed shrinkage was 27% at the completion of the hydrolysis, and the shrinkage was about 24% after the first stage. For the flow rate of 2.0 cm/min, the final shrinkage was only 13% after the first stage, and 24% after the second stage. The reaction was not completed after the second stage. At the flow rate of 0.6 cm/min, the solid bed shrank 20% after the first stage and 27% after second stage, which was the maximum observed. The reaction was indeed complete at the end of the second stage.

Analysis of Sugar Loss During Hydrolysis of Hemicellulose

Sugar produced from hemicellulose hydrolysis is subjected to decomposition. Figures 10 and 11 show how the sugar product is decomposed in each stage. The overall τ is 1.5 for the two-stage operation (τ = 0.75 for each stage). With u = 0.2 cm/min, about 2.3% sugar is decomposed in

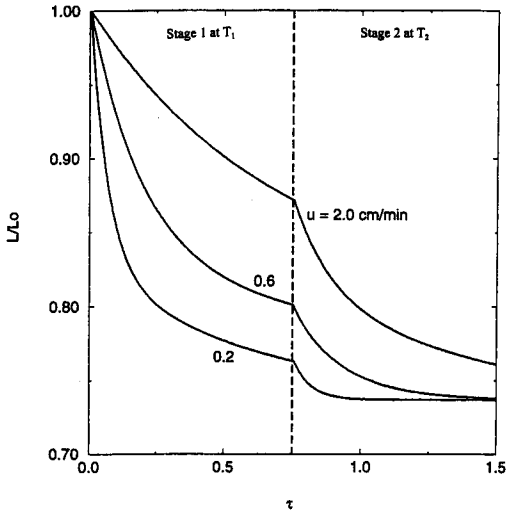

Fig. 9. Effect of acid flow rate (u) on bed shrinking (L/L_o). (T_1 = 140°C, T_2 = 170°C, L_o = 15.24 cm, C_o = 3.333 w/v%, and acid concentration = 0.8%).

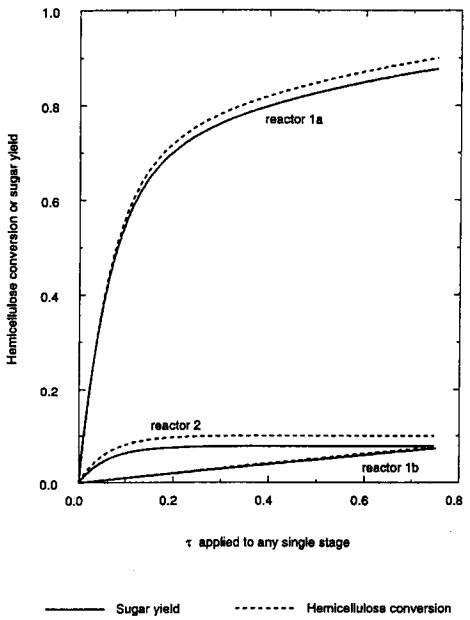

Fig. 10. Sugar decomposition at each stage during hydrolysis of hemicellulose. (T_1 = 140°C, T_2 = 170°C, L_o = 15.24 cm, C_o = 3.333 w/v%, u = 0.2 cm/min, and acid concentration = 0.8%).

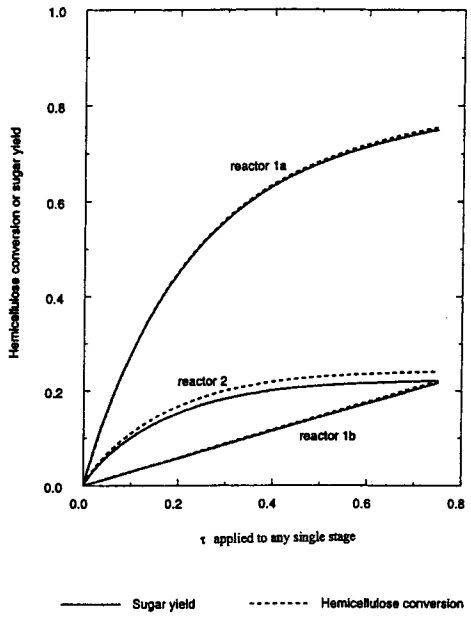

Fig. 11. Sugar decomposition at each stage during hydrolysis of hemicellulose. (T_1 = 140°C, T_2 = 170°C, L_o = 15.24 cm, C_o = 3.333 w/v%, u = 0.6 cm/min, and acid concentration = 0.8%).

Reactor A1, a reactor packed with fresh biomass at low temperature (refer to Fig. 3B for Reactors A1, A2, and B). About 2.7% sugar is decomposed in Reactor B, a reactor packed with treated biomass at high temperature. There is only a trace amount of sugar loss from Reactor A2, an artificial reactor without solid biomass. For the optimum run of u = 0.6 cm/min, there is about 2% sugar loss from Reactor B, and much less in Reactors A1 and A2. The improved performance is attributed to the low-temperature condition in Reactor A1.

CONCLUSIONS

A modeling and simulation was performed on the shrinking-bed, two-stage, reverse-flow reactor operating for dilute-acid pretreatment of CCSM. The simulation results showed that the shrinking-bed operation increases the sugar yield by about 5%, compared to the nonshrinking-bed operation at a representative τ value of 1.0. The flow rate has emerged as an important parameter acutely affecting the performance of the two-stage reactor. A simulated optimal run at τ = 1.5 reveals that fast portion of hemicellulose is almost completely hydrolyzed after the first-stage reaction. Most of the slow portion of hemicellulose is hydrolyzed in the second stage. The simulation results further prove that the two-stage operation is well suited for hydrolysis of biphasic substrates, including hemicellulose in CCSM. With application of optimal flow rates, the bed-shrinkage reached a maximum of 27%, giving almost complete conversion of hemicellulose in

CCSM. The corresponding yield was over 95%. About three-quarters of the total shrinkage occurred after the first stage. Almost all the sugar decomposition occurred at the second stage (the high-temperature reactor).

ACKNOWLEDGMENTS

This research was conducted as a part a subcontract from NREL (No. XAW-3-13441-01). Additional support was provided by the Engineering Experiment Station of Auburn University.

NOMENCLATURE

C_0	initial xylan concentration in percolation, %
H	concentration of hemicellulose as xylose in the reactor
k_{0i}	frequency factor for k_i
k_i	rate constant = $A^{ni}k_{oi}\exp(E_i/RT)$, min^{-1}. A is acid concentration.
L	reactor length, cm
t	time, min
u	velocity inside percolation reactor, cm/min
V	reactor volume
Y	yield
β_i	dimensionless reaction rate, k_iL/u
γ	ratio of solubilized lignin to solubilized hemicellulose
η	composition of hemicellulose in solid biomass
θ	conversion of hemicellulose during hydrolysis
ξ	shrinking factor, the ratio of the reactor volume after a compression operation to that of before the compression operation
τ	dimensionless residence time, tu/L
ρ	biomass density, g/mL
0	value at t = 0
ns	nonshrinking-bed operation
overall	overall value based on initial condition
s	shrinking-bed operation
i	*i*th operation
j	*j*th operation

REFERENCES

1. Lee, Y. Y., Lin, C. M., Johnson, T., and Chambers, R. P. (1978), *Biotechnol. Bioeng. Symp.* **8,** 75–88.
2. Limbaugh, M. L. (1980), MS Thesis, Auburn University, AL.
3. Cahela, D. R., Lee, Y. Y., and Chambers, R. P. (1983), *Biotechnol. Bioeng.* **25,** 3–17.
4. Kim, B. J., Lee, Y. Y., and Torget, R. W. (1993), *Appl. Biotechnol. Bioeng.* **39,** 119–129.
5. Chen, R., Lee, Y. Y., and Torget, R. W. (1996), *Appl. Biotechnol. Bioeng.* **57/58,** 133–146.
6. Torget, R. W., Hayward, T. K., Hatzis, C., and Philippidis, G. P. (1996), *Appl. Biotechnol. Bioeng.* **57/58,** 119–129.
7. Torget, R. W., Hayward, T. K., and Elander, R. (1997), *Nineteenth Symposium on Biotechnology for Fuels and Chemicals, paper No. 4* Colorado Springs, CO.
8. Chen, R. (1997), PhD Dissertation, Auburn University, AL.